

# A Neanderthal OAS1 isoform Protects Against COVID-19 Susceptibility and Severity: Results from Mendelian Randomization and Case-Control Studies

Sirui Zhou<sup>1,2,\*</sup>, Guillaume Butler-Laporte<sup>1,2,\*</sup>, Tomoko Nakanishi<sup>1,3,4,5,\*</sup>, David Morrison<sup>1</sup>, Jonathan Afilalo<sup>1</sup>, Marc Afilalo<sup>1</sup>, Laetitia Laurent<sup>1</sup>, Maik Pietzner<sup>6</sup>, Nicola Kerrison<sup>6</sup>, Kaiqiong Zhao<sup>1,2</sup>, Elsa Brunet-Ratnasingham<sup>7</sup>, Danielle Henry<sup>1</sup>, Nofar Kimchi<sup>1</sup>, Zaman Afrasiabi<sup>1</sup>, Nardin Rezk<sup>1</sup>, Meriem Bouab<sup>1</sup>, Louis Petitjean<sup>1</sup>, Charlotte Guzman<sup>1</sup>, Xiaoqing Xue<sup>1</sup>, Chris Tselios<sup>1</sup>, Branka Vulesevic<sup>1</sup>, Olumide Adeleye<sup>1</sup>, Tala Abdullah<sup>1</sup>, Noor Almamlouk<sup>1</sup>, Yiheng Chen<sup>1</sup>, Michaël Chassé<sup>7</sup>, Madeleine Durand<sup>7</sup>, Michael Pollak<sup>1</sup>, Clare Paterson<sup>8</sup>, Hugo Zeberg<sup>9</sup>, Johan Normark<sup>10</sup>, Robert Frithiof<sup>11</sup>, Miklós Lipcsey<sup>12,13</sup>, Michael Hultström<sup>11,13</sup>, Celia M T Greenwood<sup>1,2</sup>, Claudia Langenberg<sup>6,14</sup>, Elin Thysel<sup>15</sup>, Vincent Mooser<sup>3</sup>, Vincenzo Forgetta<sup>1</sup>, Daniel E. Kaufmann<sup>7,16</sup>, J Brent Richards<sup>1,2,3,17</sup>

## Affiliations:

- 1) Lady Davis Institute, Jewish General Hospital, McGill University, Montréal, Québec, Canada
- 2) Department of Epidemiology, Biostatistics and Occupational Health, McGill University, Montréal, Québec, Canada
- 3) Department of Human Genetics, McGill University Montréal, Québec, Canada
- 4) Kyoto-McGill International Collaborative School in Genomic Medicine, Graduate School of Medicine, Kyoto University, Kyoto, Japan
- 5) Research Fellow, Japan Society for the Promotion of Science
- 6) MRC Epidemiology Unit, University of Cambridge School of Clinical Medicine, Cambridge, UK
- 7) Division of Infectious Diseases and Research Centre of the Centre Hospitalier de l'Université de Montréal, Montréal, Canada
- 8) SomaLogic, Inc., Boulder, Colorado, USA
- 9) Department of Neuroscience, Karolinska Institutet, Stockholm, Sweden
- 10) Molecular Infection Medicine Sweden (MIMS), Umeå University
- 11) Anaesthesiology and Intensive Care Medicine, Department of Surgical Sciences, Uppsala University, Uppsala, Sweden.
- 12) Hedenstierna Laboratory, CIRRUS, Anaesthesiology and Intensive Care Medicine, Department of Surgical Sciences, Uppsala University, Uppsala, Sweden
- 13) Integrative Physiology, Department of Medical Cell Biology, Uppsala University, Uppsala, Sweden
- 14) Computational Medicine, Berlin Institute of Health, Charité University Medicine Berlin, Germany
- 15) Department of Medical Biosciences, Umeå University
- 16) Department of Medicine, Université de Montréal, Montréal, Canada
- 17) Department of Twin Research, King's College London, London, United Kingdom

\*These authors contributed equally to this study

## Corresponding author:

Brent Richards, Professor of Medicine, McGill University  
Senior Lecturer, King's College London (Honorary)  
Pavilion H-413, Jewish General Hospital  
3755 Côte-Ste-Catherine Montréal, Québec, Canada, H3T 1E2  
T: +1 514 340 8222 x24362 F: +1 514 340 7529  
E: [brent.richards@mcgill.ca](mailto:brent.richards@mcgill.ca) [www.mcgill.ca/genepi](http://www.mcgill.ca/genepi)

**Funding:** The Richards research group is supported by the Canadian Institutes of Health Research (CIHR: 365825; 409511), the Lady Davis Institute of the Jewish General Hospital, the Canadian Foundation for Innovation (CFI), the NIH Foundation, Cancer Research UK, Genome Québec, the Public Health Agency of Canada, the **McGill** Interdisciplinary Initiative in Infection and Immunity and the Fonds de Recherche

56 Québec Santé (FRQS). SZ is supported by a CIHR fellowship and a FRQS fellowship. GBL is supported  
57 by the a CIHR scholarship, and a joint FRQS and Québec Ministry of Health and Social Services  
58 scholarship. TN is supported by Research Fellowships of Japan Society for the Promotion of Science  
59 (JSPS) for Young Scientists. JBR is supported by a FRQS Clinical Research Scholarship. Support from  
60 Calcul Québec and Compute Canada is acknowledged. TwinsUK is funded by the Wellcome Trust, Medical  
61 Research Council, European Union, the National Institute for Health Research (NIHR)-funded  
62 BioResource, Clinical Research Facility and Biomedical Research Centre based at Guy's and St Thomas'  
63 NHS Foundation Trust in partnership with King's College London. BQC-19 is funded by FRQS, Genome  
64 Québec and the Public Health Agency of Canada. These funding agencies had no role in the design,  
65 implementation or interpretation of this study. VM is supported by a Canada Excellence Research Chair.  
66 The Kaufmann lab COVID-19 work is supported by the CIHR/CITF (VR2-173203), AmFAR (110068-68-  
67 RGCV) the CFI and FRQS. RF is supported by Swedish Research Council (2014-02569 and 2014-07606).  
68 MH is supported by a SciLifeLab/KAW national COVID-19 research program project grant (KAW  
69 2020.0182).

70

71 **Disclosures:** JBR has served as an advisor to GlaxoSmithKline and Deerfield Capital.

72

73 **Key words:** Genome-wide association studies, COVID-19, Mendelian randomization, proteomics

74

75 **Abstract**

76 Proteins detectable in peripheral blood may influence COVID-19 susceptibility or severity. However,  
77 understanding which circulating proteins are etiologically involved is difficult because their levels may be  
78 influenced by COVID-19 itself and are also subject to confounding factors. To identify circulating proteins  
79 influencing COVID-19 susceptibility and severity we undertook a large-scale two-sample Mendelian  
80 randomization (MR) study, since this study design can rapidly scan hundreds of circulating proteins and  
81 reduces bias due to reverse causation and confounding. We identified genetic determinants of 931  
82 circulating proteins in 28,461 SARS-CoV-2 uninfected individuals, retaining only single nucleotide  
83 polymorphism near the gene encoding the circulating protein. We found that a standard deviation  
84 increase in OAS1 levels was associated with reduced COVID-19 death or ventilation (N = 4,336 cases /  
85 623,902 controls; OR = 0.54, P =  $7 \times 10^{-8}$ ), COVID-19 hospitalization (N = 6,406 / 902,088; OR = 0.61, P =  
86  $8 \times 10^{-8}$ ) and COVID-19 susceptibility (N = 14,134 / 1,284,876; OR = 0.78, P =  $8 \times 10^{-6}$ ). Results were  
87 consistent in multiple sensitivity analyses. We then measured OAS1 levels in 504 patients with repeated  
88 plasma samples (N=1039) with different COVID-19 outcomes and found that increased OAS1 levels in a  
89 non-infectious state were associated with protection against very severe COVID-19, hospitalization and  
90 susceptibility. Further analyses suggested that a Neanderthal isoform of OAS1 affords this protection.  
91 Thus, evidence from MR and a case-control study supported a protective role for OAS1 in COVID-19  
92 outcomes. Available medicines, such as phosphodiesterase-12 inhibitors, increase OAS1 and could be  
93 explored for their effect on COVID-19 susceptibility and severity.

94

## 95 **Introduction**

96 To date, the COVID-19 pandemic has caused more than 1.6 million deaths worldwide, and infected over  
97 75 million individuals.<sup>1</sup> Despite the scale of the epidemic, there are at present few disease-specific  
98 therapies<sup>2</sup>. to reduce the morbidity and mortality of SARS-CoV-2 infection, and apart from  
99 dexamethasone therapy in oxygen dependent patients<sup>3</sup>, most clinical trials have shown at most mild or  
100 inconsistent benefits in disease outcome.<sup>4–6</sup> Therefore, validated targets are needed for COVID-19  
101 therapeutic development.

102

103 One source of such targets is circulating proteins. Recent advances in large-scale proteomics have  
104 enabled the measurement of thousands of circulating proteins at once and when combined with evidence  
105 from human genetics, such targets greatly improve the probability of drug development success.<sup>7–9</sup> While  
106 *de novo* drug development will take time—even in the accelerated arena of COVID-19 therapies—  
107 repurposing of currently available molecules targeting those proteins could also provide an accelerated  
108 opportunity to deliver new therapies to patients.

109

110 Nevertheless, since confounding and reverse causation often bias traditional circulating protein  
111 epidemiological studies, disentangling the causal relationship between circulating proteins and COVID-19  
112 susceptibility or severity is challenging. This is especially the case in COVID-19, where exposure to  
113 SARS-CoV-2 unleashes profound changes in circulating protein levels<sup>10</sup>. One way to address these  
114 limitations is by using Mendelian randomization (MR), a genetic epidemiology method that uses genetic  
115 variants as instrumental variables to test the effect of an exposure (here protein levels) on an outcome  
116 (here COVID-19 outcomes). Given that genotypes are determined by randomly segregated alleles during  
117 meiosis of parental gametes, this greatly reduces bias due to confounding. Since genotypes are always  
118 assigned prior to disease onset, MR studies are not influenced by reverse causation. However, MR rests  
119 on several assumptions<sup>11</sup>, the most problematic being the lack of horizontal pleiotropy of the genetic  
120 instruments (wherein the genotype influences the outcome, independently of the exposure). One way to

121 help avoid this bias is to use genetic variants that influence circulating protein levels which are adjacent to  
122 the gene which encodes the circulating protein through the use of *cis*-protein quantitative trait loci (*cis*-  
123 pQTLs).<sup>9</sup> Given their close proximity to the target gene, *cis*-pQTLs are likely to influence the level of the  
124 circulating protein, among others, by directly influencing its transcription or translation, and therefore less  
125 likely to affect the outcome of interest (COVID-19) through pleiotropic pathways. Nevertheless, a causal  
126 genetic association between the exposure and outcome may be confounded by linkage disequilibrium  
127 (LD, the non-random association of genetic variants assigned at conception).<sup>12</sup> To probe this potential  
128 problem, colocalization tests can assess for the presence of bias from LD.

129

130 Understanding the etiologic role of circulating proteins in infectious diseases is challenging because the  
131 infection itself often leads to large changes in circulating protein levels<sup>10</sup>. Thus, it may appear that an  
132 increase in a circulating protein, such as a cytokine, is associated with a worsened outcome, when in fact,  
133 the cytokine may be the host's response to this infection and help to mitigate this outcome. It is therefore  
134 important to identify genetic determinants of the protein levels in the non-infected state, which would  
135 reflect a person's baseline predisposition to the level of a protein.

136

137 MR studies can be complemented by traditional case-control studies, where the protein is longitudinally  
138 measured in COVID-19 patients and controls, allowing for an estimation of the association between the  
139 protein level and COVID-19 outcomes. However, MR studies would tend to predict the effect of the  
140 protein in the non-infectious state when the genetic determinants of such proteins are measured in the  
141 non-infected population. Thus, longitudinal measurements of proteins can allow for a better  
142 understanding of the role of such proteins in COVID-19 outcomes and also describe how their levels  
143 respond to the infection. Since MR and case-control studies rely on different assumptions, and may be  
144 influenced by different biases, concordant results between the two study designs can strengthen the  
145 cumulative evidence through the concept of the triangulation of evidence<sup>13</sup>.

146

147 In this study, we therefore undertook two-sample MR and colocalization analyses to combine results from  
148 large-scale genome-wide association studies (GWAS) of circulating protein levels and COVID-19  
149 outcomes<sup>14</sup> in order to prioritize proteins likely influencing COVID-19 outcomes. We began by identifying  
150 the genetic determinants of circulating protein levels in large-scale protein level GWASs, then used MR to  
151 assess whether these *cis*-pQTLs were associated with COVID-19 outcomes in the ICDA Host Genetics  
152 Initiative COVID-19 outcomes GWASs. Next, we investigated expression QTL (eQTL) and splice QTL  
153 (sQTL) effects of our lead proteins. We then measured the most promising protein, OAS1, in 504 subjects  
154 ascertained for SARS-CoV-2 infection and when PCR positive, followed for longitudinal sampling during  
155 and after their infection.

156

## 157 **Results**

### 158 ***MR using cis-pQTLs, and pleiotropy assessment***

159 Study design is illustrated in **Figure 1**. We began by obtaining the genetic determinants of circulating  
160 protein levels from six large proteomic GWAS of European individuals (Sun *et al*<sup>15</sup> N=3,301; Emilsson *et*  
161 *al*<sup>16</sup> N=3,200; Pietzner *et al*<sup>17</sup> N=10,708; Folkersen *et al*<sup>18</sup> N=3,394; Yao *et al*<sup>19</sup> N=6,861 and Suhre *et al*<sup>20</sup>  
162 N=997). A total of 931 proteins from these six studies had *cis*-pQTLs associated at a genome-wide  
163 significant level ( $P < 5 \times 10^{-8}$ ) with protein levels, or highly correlated proxies ( $LD R^2 > 0.8$ ), in the meta-  
164 analyses of data from the COVID-19 Host Genetics Initiative<sup>21</sup> which included results from the  
165 GenOMICC program<sup>22</sup>. We then undertook MR analyses using 1,425 directly matched *cis*-pQTLs and 39  
166 proxies as genetic instruments across six studies for their associated circulating proteins on three  
167 separate COVID-19 outcomes: 1) Very severe COVID-19 disease (defined as individuals experiencing  
168 death, mechanical ventilation, non-invasive ventilation, high-flow oxygen, or use of extracorporeal  
169 membrane oxygenation. 99.7% of these individuals were of European ancestry) using 4,336 cases and  
170 623,902 controls; 2) COVID-19 disease requiring hospitalization using 6,406 cases and 902,088 controls  
171 of European ancestry and 3) COVID-19 susceptibility using 14,134 cases and 1,284,876 controls of  
172 European ancestry. These case-control phenotype definitions are referred to as A2, B2, and C2 by the  
173 COVID-19 Host Genetics Initiative, respectively. In all outcomes, cases required evidence of SARS-CoV-

174 2 infection. For the very severe COVID-19 and hospitalization outcomes, COVID-19 cases were defined  
175 as laboratory confirmed SARS-CoV-2 infection based on nucleic acid amplification or serology tests. For  
176 the COVID-19 susceptibility outcome, cases were also identified by review of health records (using  
177 International Classification of Disease codes or physician notes).

178

179 MR analyses revealed that the levels of three circulating proteins, 2'-5'-oligoadenylate synthetase 1  
180 (OAS1), interleukin-10 receptor beta subunit (IL10RB) and ABO were associated with at least two  
181 COVID-19 outcomes after Benjamini & Hochberg FDR correction for the number of proteins tested (**Table**  
182 **1, Tables S1-6**). We note that FDR correction is overly conservative given the non-independence of the  
183 circulating protein levels. Notably, increased OAS1 levels were strongly associated with protection from  
184 all three COVID-19 outcomes. Further, these effect sizes were more pronounced in severe and  
185 hospitalization outcomes, such that each standard deviation increase in OAS1 levels was associated with  
186 decreased odds of very severe COVID-19 (OR=0.54; 95% CI: 0.44-0.68,  $P=7.0 \times 10^{-8}$ ), hospitalization  
187 (OR=0.61; 95% CI: 0.51-0.73,  $P=8.3 \times 10^{-8}$ ) and susceptibility (OR=0.78; 95% CI: 0.69-0.87,  $P=7.6 \times 10^{-6}$ )  
188 (**Figure 2A**). We also identified OAS1 *cis*-pQTLs in Emilsson *et al*<sup>16</sup> and Pietzner *et al*<sup>17</sup> which were not  
189 included in the MR analyses due to lack of genome-wide significance in their association with OAS1  
190 levels or missing from initial protein panel. Undertaking MR analyses of using these additional *cis*-pQTLs,  
191 we found concordant results (**Table S7**).

192

193 We next assessed whether the *cis*-pQTL associated with OAS1 levels (rs4767027) was associated with  
194 any other phenotypes across more than 5,000 outcomes, as catalogued in PhenoScanner,<sup>23</sup> which  
195 collects associations of SNPs with outcomes from all available GWASs. We found that the only significant  
196 association for rs4767027 was with circulating OAS1 levels ( $P=6.2 \times 10^{-26}$ ) in plasma, whereas it was not  
197 associated with any other traits or protein levels ( $P<5.0 \times 10^{-5}$ ). These findings reduce the possibility that  
198 the MR estimate of the effect of OAS1 on COVID-19 outcomes is due to horizontal pleiotropy. Finally,  
199 except for the susceptibility outcome, the effect of rs4767027 did not demonstrate evidence of  
200 heterogeneity across COVID-19 Host Genetics Initiative GWAS meta-analyses (**Table 1**).

201

202 We next identified an independent SNP associated with OAS1 circulating protein levels, which was not at  
203 the *OAS1* locus and is thus a *trans*-SNP (rs62143197, P value for association with OAS1 levels =  $7.10 \times$   
204  $10^{-21}$ ). However, this SNP is likely subject to pleiotropic effects, since it is strongly associated with many  
205 other proteins, such as annexin A2 ( $P=5.6 \times 10^{-237}$ ) and small ubiquitin-related modifier 3 ( $P=9.1 \times 10^{-178}$ ).  
206 Consequently, including this *trans*-SNP could introduce bias from horizontal pleiotropic effects and was  
207 thus not considered in further MR analyses. Further, this trans-association signal was unique to the  
208 INTERVAL study<sup>17</sup>.

209

210 OAS proteins are part of the innate immune response against RNA viruses. They are induced by  
211 interferons and activate latent RNase L, resulting in direct viral and endogenous RNA destruction, as  
212 demonstrated in *in-vitro* studies.<sup>24</sup> Thus OAS1 has a plausible biological activity against SARS-CoV-2.

213

214 Using a *cis*-pQTL for IL10RB (rs2834167), we found that one standard deviation increase in circulating  
215 IL10RB level was associated with decreased odds for very severe COVID-19 (OR=0.47; 95% CI: 0.32-  
216 0.68,  $P=7.1 \times 10^{-5}$ ) and hospitalization (OR = 0.53; 95% CI: 0.39-0.73,  $P=8.8 \times 10^{-5}$ ). However, circulating  
217 IL10RB protein level was not associated with COVID-19 susceptibility. Using PhenoScanner, we could  
218 not find evidence of pleiotropic effects of the *cis*-pQTL for IL10RB. The IL10RB *cis*-pQTL also showed a  
219 homogeneous effect across the three COVID-19 outcomes except for susceptibility to COVID-19 (**Table**  
220 **1, Figure 2A**). MR revealed that one standard deviation increase in circulating ABO level was associated  
221 with increased odds of adverse COVID-19 outcomes (**Table 1**), however, we found that a *cis*-pQTL for  
222 ABO (rs505922) was strongly associated with the levels of several other proteins, suggesting potential  
223 horizontal pleiotropic effects (**Table S8**). Given ABO's known involvement in multiple physiological  
224 processes, these results were expected, but highlight that MR analyses may suffer from significant bias  
225 from horizontal pleiotropy.

226



## 227 **Colocalization Studies**

228 To test whether confounding due to LD may have influenced the estimated effect of circulating OAS1 on  
229 the three different COVID-19 outcomes, we tested the probability that the genetic determinants of OAS1  
230 circulating protein level were shared with the three COVID-19 outcomes using colocalization analyses.  
231 These were performed using *coloc*, a Bayesian statistical test implemented in the *coloc* R package.<sup>12</sup> We  
232 found that the posterior probability that OAS1 levels and COVID-19 outcomes shared a single causal  
233 signal (the posterior probability for hypothesis 4 in *coloc*, PP4) in the 1Mb locus around the cis-pQTL  
234 rs4767027 was 0.72 for very severe COVID-19, 0.82 for hospitalization due to COVID-19, and 0.89 for  
235 COVID-19 susceptibility (**Figure 3**). This colocalization result was also replicated using cis-pQTLs for  
236 OAS1 levels identified by Pietzner *et al*<sup>17</sup> (**Table S7**). This suggests that there is likely a single shared  
237 causal signal for OAS1 circulating protein levels and COVID-19 outcomes.

238

239 Colocalization of ABO levels and different COVID-19 outcomes also showed colocalization between ABO  
240 level and different COVID-19 outcomes (posterior probability of single shared signal = 0.90, 0.98 and 1 for  
241 ABO level and very severe COVID-19, hospitalization due to COVID-19 and susceptibility, respectively)  
242 (**Figure S1**). We were unable to perform colocalization analyses for IL10RB due to a lack of genome-wide  
243 summary level data from the original proteomic GWAS<sup>16</sup>.

244

## 245 **Aptamer Binding Effects**

246 Protein altering variants (PAVs)<sup>15</sup> may influence binding of affinity agents, such as aptamers or  
247 antibodies, that are used to quantify protein levels. We thus assessed if the cis-pQTLs for the MR-  
248 prioritized proteins were PAVs, or in LD ( $R^2 > 0.8$ ) with PAVs, and if so, whether conditioning the cis-  
249 pQTLs on correlated PAVs influenced their association with COVID-19 outcomes. rs2834167 (IL10RB) is  
250 a nonsense variant and could therefore be subject to potential binding effects. rs505922 (ABO) is not in  
251 LD with known missense variants. rs4767027 (OAS1) is an intronic variant, which is in LD with a  
252 missense variant rs2660 ( $R^2 = 1$ ) in European ancestry. Unfortunately, this missense variant was not

253 included in the imputation data of Sun *et al*, and the effect by this missense variant could not be  
254 evaluated. However, since RNA splicing and expression studies derived from RNA sequencing are not  
255 subject to potential effects of missense variants that could influence aptamer binding, we next explored  
256 whether rs4767027 also influences OAS1 splicing and/or expression.

257

### 258 ***sQTL and eQTL studies for OAS genes***

259 Splicing QTLs (sQTLs) are genetic variants that influence the transcription of different isoforms of a  
260 protein. The aptamer that targets OAS1 was developed against a synthetic protein comprising the amino  
261 acid sequence 1-364 of NP002525.<sup>25</sup>, which is common to the two major OAS1 isoforms, p46 and p42,  
262 and hence the aptamer may identify both, or either isoforms. rs10774671 is a known sQTL for OAS1 that  
263 induces alternate splicing and create p46 and p42, a majority of present-day people carry this splice  
264 variant (rs10774671-A), which increases expression of isoforms other than p46<sup>26</sup>. The ancestral variant  
265 (rs10774671-G) is the major allele in African populations and became fixed in Neanderthal and  
266 Denisovan genomes<sup>27,28</sup>. However, the ancestral variant, with its increased expression of the p46 isoform,  
267 was reintroduced into the European population via gene flow from Neanderthals<sup>29</sup>, and is also the  
268 predominant isoform found in circulating blood<sup>26</sup>. The p46 isoform has been demonstrated to have higher  
269 anti-viral activity than other isoforms<sup>30</sup>. Interestingly, the OAS1 pQTL, rs4767027, is in high LD ( $R^2=0.97$ )  
270 with rs10774671<sup>29</sup> in European populations. Functional studies support that the G allele at rs10774671  
271 increases expression of the p46 isoform but decreases expression of the p42 isoform<sup>26</sup>. This G allele at  
272 the sQTL rs10774671 reflects the T allele at pQTL rs4767027, which itself is associated with higher  
273 measured OAS1 levels and reduced odds of COVID-19 severity and susceptibility. These separate lines  
274 of evidence suggest that the p46 isoform was predominantly measured by the SomaScan® platform and  
275 may protect against COVID-19 outcomes.

276

277 Undertaking MR studies of OAS1 splicing, we found that increased expression of the p46 isoform (as  
278 defined by normalized read counts of the intron cluster defined by LeafCutter<sup>31,32</sup>) was associated with

279 reduced odds of COVID-19 outcomes (OR = 0.29; 95% CI: 0.17-0.49,  $P=4.1 \times 10^{-6}$  for susceptibility, OR =  
280 0.09; 95% CI: 0.04-0.21,  $P=2.0 \times 10^{-8}$  for hospitalization and OR = 0.05; 95% CI: 0.02-0.13,  $P=3.1 \times 10^{-9}$  for  
281 very severe COVID-19) (**Figure 2B**). Colocalization analyses also supported a shared causal signal  
282 between the sQTL for *OAS1*, the pQTL and COVID-19 outcomes (**Figure S2A-B**). Interestingly, the  
283 colocalization analyses supported a stronger probability of a shared signal with the sQTL, than the pQTL,  
284 suggesting that the p46 isoform may be the driver of the association of *OAS1* levels with COVID-19  
285 outcomes.

286

287 Next, we tested whether increased expression of *OAS1* levels, without respect to isoform, were  
288 associated with COVID-19 outcomes using eQTL MR analyses. We identified an expression QTL (eQTL)  
289 for total *OAS1*, rs10744785, from GTEx v8.<sup>33</sup> Total *OAS1* expression levels were not associated with  
290 COVID-19 susceptibility and hospitalization (**Figure 2B**). We also found that increased *OAS3* expression  
291 level in whole blood was positively associated with COVID-19 outcomes in MR analyses with a support  
292 for colocalization of their genetic signal (**Table S9, Figure S3**).

293

294 Taken together, these pQTL, sQTL and eQTL studies suggest that increased levels of the p46 isoform of  
295 *OAS1* protect against COVID-19 adverse outcomes. Further, the concordant evidence from sQTL and  
296 pQTL MR studies suggest that the effect of *OAS1* levels on COVID-19 outcomes is unlikely to be biased  
297 by aptamer binding effects.

298

### 299 *Association of measured OAS1 protein level with COVID-19 outcomes*

300 Since MR studies were derived from protein levels measured in a non-infected state, we tested the  
301 hypothesis that increased *OAS1* protein levels in a non-infected state would be associated with reduced  
302 odds of COVID-19 outcomes. To do so, we undertook a case-control study, measuring *OAS1* protein  
303 levels using the SomaScan® platform in 1039 longitudinal samples from 399 SARS-CoV-2 PCR positive  
304 patients collected at multiple time points during their COVID-19 infection and 105 individuals who

305 presented with COVID-19 symptoms but had negative SARS-CoV-2 PCR nasal swabs from the  
306 Biobanque Quebecoise de la COVID-19 cohort ([www.BQC19.ca](http://www.BQC19.ca)). Individuals were recruited  
307 prospectively who had undergone nasal swabs for SARS-CoV-2 infection. The demographic  
308 characteristics of the participants in the BQC19 cohort who underwent SomaScan® assays is detailed in  
309 **Table 2**.

310

311 We defined non-infectious samples as those collected from convalescent SARS-CoV-2 patients at least  
312 31 days after onset of their symptoms (N=115), or samples collected from SARS-CoV-2 PCR negative  
313 patients (N=105). These SARS-CoV-2 PCR negative patients were recruited as controls into the study, as  
314 their inclusion reduces the probability of the introduction of collider bias<sup>34</sup>. As we also observed a change  
315 in OAS1 level with the exposure to the SARS-CoV-2 virus (**Figure S4**), in order to understand how OAS1  
316 protein levels during infection would be associated with COVID-19 outcomes, we also measured OAS1  
317 levels in individuals with samples from SARS-CoV-2 positive patients <14 days after symptom onset  
318 (N=313). Sample outliers were removed (**Figure S5, S6**), and we showed that OAS1 levels are not  
319 associated with age and sex in samples without active infection (**Figure S7**). Additional sample QC and  
320 characterization of the cohort is described in **Supplementary data**.

321

322 To test whether OAS1 levels in a non-infectious state were associated with COVID-19 outcomes we  
323 undertook logistic regression using the three COVID-19 outcomes, while controlling for age, sex, age<sup>2</sup>,  
324 plate, recruitment center and sample processing time. OAS1 levels were log-transformed and  
325 standardized to match the transformation procedure of the MR study. We found that in the non-infectious  
326 samples, each standard deviation increase in OAS1 levels on the log-transformed scale was associated  
327 with reduced odds of COVID-19 outcomes (OR = 0.20 [95% CI: 0.08 – 0.53]; P = 0.001 for very severe  
328 COVID-19, OR = 0.46 [95% CI: 0.28 – 0.76], P = 0.002 for hospitalization and OR = 0.69 [95% CI: 0.49 –  
329 0.98], P = 0.04 for susceptibility) (**Figure 4, Table S10, Figure S8**). These results are consistent with our  
330 findings from MR, where increased circulating OAS1 levels in a non-infectious state were associated with  
331 protection against all of these adverse COVID-19 outcomes.

332

333 In samples drawn during active infection we found that increased OAS1 levels were associated with  
334 increased odds of adverse COVID-19 outcomes (OR = 1.49 [95% CI: 1.19 – 1.90]; P = 0.0007 for very  
335 severe COVID-19, OR = 1.92 [95% CI: 1.46 – 2.56], P =  $4.8 \times 10^{-6}$  for hospitalization and OR = 4.39 [95%  
336 CI: 2.87 – 6.73], P =  $1.09 \times 10^{-11}$  for susceptibility) (**Figure 4, Table S10, Figure S8**).

337

338 Taken together, these findings suggest that increased OAS1 levels in a non-infectious state are  
339 associated with better COVID-19 outcomes, and that during infection, SARS-CoV-2 exposure likely  
340 causes OAS1 levels to increase, as interferon pathways are stimulated, which are known to increase  
341 OAS1 levels<sup>35</sup>.

342

### 343 **Discussion:**

344 Disease-specific therapies are needed to reduce the morbidity and mortality associated with COVID-19  
345 outcomes. In this large-scale two-sample MR study of 931 proteins assessed for three COVID-19  
346 outcomes in up to 14,134 cases and 1.2 million controls with European ancestry, we provide evidence  
347 that increased OAS1 levels in the non-infectious state are strongly associated with reduced risks of very  
348 severe COVID-19, hospitalization and susceptibility. The protective effect size was particularly large, such  
349 that a 50% decrease in the odds of very severe COVID-19 was observed per standard deviation increase  
350 in OAS1 circulating levels. Since therapies exist that activate OAS1, repositioning them as potential  
351 COVID-19 treatments should be prioritized.

352

353 In non-Sub-Saharan African populations, the protective alleles at both rs4767027-T (the OAS1 pQTL) and  
354 rs10774671-G (the OAS1 sQTL) are found on a Neandertal haplotype which was passed on to modern  
355 humans ~50-60,000 years ago<sup>36</sup>. Even though these two SNPs share a haplotype, their evolutionary  
356 histories differ. The rs4767027-T allele is derived from the Neandertal lineage, whereas for the  
357 rs10774671-G allele, Neanderthals preserved the ancestral state. OAS1 alternative splicing regulated by

358 the rs10774671-G allele increases the isoform p46, which is known to have a higher enzymatic activity  
359 against viruses than the p42 isoform<sup>37</sup>. p46 is also known to be the only OAS1 isoform which is robustly  
360 upregulated during infection<sup>29</sup>. Although further studies are needed to fully elucidate the functional  
361 relevance of the pQTL and sQTL for OAS1, the antiviral activity of the gene products is higher for the  
362 Neandertal haplotype than the common haplotype in Europeans<sup>30</sup>. In Europeans the Neandertal  
363 haplotype has undergone positive selection<sup>29</sup> and the rs4767027-T allele reaches an allele frequency of  
364 0.32, whereas it is absent in sub-Saharan African populations. The association between the Neanderthal  
365 haplotype and protection against severe COVID-19 was recently described<sup>38</sup>. Using MR and  
366 measurements of circulating proteins, we demonstrated here that increased OAS1 levels of the  
367 Neandertal haplotype confers this protective effect.

368

369 Our MR evidence indicated that higher p46 isoform levels of OAS1 and higher OAS1 total protein levels,  
370 as measured by the SomaScan<sup>®</sup> assay had protective effects on COVID-19 outcomes. These results  
371 were strongly supported by colocalization analysis. Given the consistent colocalization between the sQTL  
372 and pQTL for OAS1, the lack of colocalization between the eQTL and pQTL for OAS1, and the evidence  
373 that the SomaScan<sup>®</sup> assay likely measures p46 isoforms, rather than total protein levels, it seems  
374 probable that the protective effect of OAS1 is derived from the p46 isoform. However, further  
375 investigations are required to specifically measure each isoform in circulation.

376

377 In light of the protective effect of the ancestral OAS1 splice variant (rs10774671-G) on COVID-19 and the  
378 positive selection of the Neandertal haplotype in Europeans, the loss-of-function variant (rs10774671-A)  
379 found in non-African population is surprising. Several scenarios might explain this loss-of-function, e.g.,  
380 loss of purifying selection during the out-Africa exodus due to changes in environmental pathogens.  
381 Moreover, immune responses can be harmful and loss-of-function in OAS1-antiviral activity has been  
382 observed in several primates<sup>39</sup>, suggesting a cost of OAS1 activity. Nevertheless, our results indicate that  
383 interbreeding between Neanderthals and modern humans confers some protection against COVID-19.

384 The OAS1 Neanderthal variant is another risk-modulating locus reported to be inherited from  
385 Neanderthals, the other being the chromosome 3 risk locus<sup>40</sup>.

386

387 *OAS1*, *OAS2* and *OAS3* share significant homology and differ only in their number of OAS units. They  
388 also increase expression of both IRF3 and IRF7, both genes involved in interferon-induced gene  
389 expression. As an interferon stimulated gene<sup>41</sup>, *OAS1* polymorphisms have been associated with the host  
390 immune response to several classes of viral infection including influenza<sup>42</sup>, herpes simplex<sup>43</sup>, hepatitis C ,  
391 West Nile<sup>44</sup> Dengue<sup>45</sup>, and SARS-CoV<sup>46</sup> viruses. Given that *OAS1* is an intracellular enzyme leading to  
392 viral RNA degradation, it is probable that the circulating levels of this enzyme reflect intracellular levels of  
393 this protein. However, there exists considerable evidence that circulating *OAS1* is also important in the  
394 viral immune response<sup>47</sup>.

395

396 Molecules currently exist which can increase *OAS1* activity. Interferon beta-1b, which activates a cytokine  
397 cascade leading to increased *OAS1* expression,<sup>48</sup> is currently used to treat multiple sclerosis and has  
398 been shown to induce *OAS1* expression in blood.<sup>49</sup> Interferon-based therapy has also been used in other  
399 viral infections<sup>50</sup>. However, recent randomized trials have shown inconsistent results. While intravenous  
400 interferon beta-1b combined with lopinavir-ritonavir reduced mortality due to MERS-CoV infections,<sup>51</sup> in  
401 the unblinded SOLIDARITY trial,<sup>52</sup> there was no demonstrated benefit of intravenous interferon-beta-1b.  
402 On the other hand, a recent phase II trial testing the effect of inhaled nebulized interferon beta-1b showed  
403 improved symptoms in the treatment arm.<sup>53</sup> While this study was not powered to show a difference in  
404 mortality, all deaths occurred in the placebo group. Inhaled nebulized interferon-1-beta results in a much  
405 higher tissue availability in the lung and may result in improved anti-viral activity. Moreover, timing of  
406 administration is likely to play a role, as the administration of a pro-inflammatory cytokine may not provide  
407 benefit during the inflammation driven phase of the disease. However, data on timing of administration is  
408 currently unavailable in the SOLIDARITY trial, and conclusions cannot yet be drawn. Lastly the effect of  
409 interferon supplement may vary across ancestral population, as different ancestries have different  
410 amounts of the more active p46 isoform of *OAS1*. Our study was limited to individuals of European

411 ancestry, a population with higher expression of the p46 isoform. Interestingly, the SOLIDARITY trial  
412 enrolled 61% of its patients in Africa or Asia, and 17% in Latin America, populations with higher  
413 expression of the p42 isoform OAS1, while the study on inhaled interferon beta-1b was comprised of 80%  
414 White patients from the United Kingdom. This suggests that interferon beta-1b may have different effects  
415 in populations of different ancestry, due to presence of different genetic variants.

416

417 *In-vitro* evidence also exists demonstrating that pharmacological inhibition of phosphodiesterase-12,  
418 which normally degrades the OAS enzymes, potentiates this OAS-mediated antiviral activity.<sup>54</sup> PDE-12  
419 inhibitors potentiate the action of OAS1, 2 and 3.<sup>55</sup> Interestingly other coronaviruses in the same  
420 betacoronavirus family as SARS-CoV-2 have been shown to produce viral proteins that degrade the OAS  
421 family of proteins, and antagonize RNase-L activity, leading to evasion of the host immune response.<sup>56,57</sup>  
422 Thus classes of medications currently exist that lead to increased OAS1 levels and could be explored for  
423 their effect upon COVID-19 outcomes.

424

425 Our MR analyses found that higher level of OAS3 expression is associated with worse COVID-19  
426 outcomes, which is an opposite direction of effect compared to OAS1. The discordant effects of the  
427 Neanderthal haplotype for OAS1 and OAS3 were also reported by a previous study<sup>29</sup> , which might reflect  
428 complex biology of OAS genes for innate immune response. In a recent transcription-wide association  
429 study from the GenOMICC program<sup>22</sup>, genetically-predicted high expression of OAS3 in lungs and whole  
430 blood were associated with higher risk of becoming critically ill COVID-19 patients. Although further  
431 studies to assess the roles of OAS genes specific to SARS-CoV-2 are needed, it is likely that OAS1 is the  
432 main driver of the protective effect of Neanderthal haplotype for COVID-19 outcomes given prior  
433 functional studies demonstrating the antiviral effect of OAS genes<sup>29</sup>.

434

435 *IL10RB* encodes for the beta subunit of the IL10 receptor (a type III interferon receptor), and is part of a  
436 cluster of immunologically important genes including *IFNAR1* and *IFNAR2*, both recently implicated in



437 severe COVID-19 pathophysiology.<sup>58</sup> *IFNAR1* and 2 encode the interferon alpha/beta receptor subunits 1  
438 and 2, respectively. Interestingly, while there exists a *cis*-pQTL strongly associated with *IFNAR1* levels, it  
439 was not associated with any of the COVID-19 outcomes ( $P \sim 0.5$ ). Further, *IFNAR1* had no *trans*-pQTLs  
440 identified, which means that the *IL10RB cis*-pQTL does not likely reflect *IFNAR1* levels. However, since  
441 *IFNAR2* was not measured in any proteomic studies, we could not test the effect of its circulating levels  
442 on COVID-19 outcomes. *IL10RB* mediates *IL10* anti-inflammatory activity through its downstream  
443 inhibitory effect on many well-known pro-inflammatory cytokines such as janus kinases and *STAT1*.<sup>59</sup>  
444 While overexpression of *IL10* has been involved in the persistence of multiple chronic bacterial infections  
445 such as tuberculosis,<sup>60</sup> its role remains poorly understood in acute infections. In sepsis, a disease state  
446 characterized by high levels of cytokine activity and a rise in multiple biomarkers associated with  
447 inflammation, there is also a well-established increase in anti-inflammatory *IL10* production by leukocytes,  
448 especially in the early stage of the disease.<sup>61</sup> Most importantly, while in a normal physiological state, *IL10*  
449 is usually only produced at a low level by neutrophils, monocytes and macrophages, its production is  
450 strongly upregulated by *IL4*, itself upregulated by lipopolysaccharides (*LPS*) when they bind *LBP*s.<sup>62,63</sup>  
451 Interestingly, while the *LBP* gene did not pass FDR correction, it was still one of the most significant  
452 protein in our MR *cis*-pQTL analysis (**Table S1, S3**). While *LPS*'s are well-known for their role in triggering  
453 gram-negative bacterial sepsis, their role in other acute infections and respiratory diseases is likely  
454 broader, and involves complex sequences of cytokine signaling.<sup>64-67</sup> Nevertheless, as our MR studies  
455 showed that *IL10RB* protein level affected COVID-19 outcome with a concordant effect direction, and  
456 given the known role of overt inflammation in COVID-19 morbidity, this pathway likely deserves more  
457 investigation.

458

459 This study has limitations. First, we used MR to test the effect of circulating protein levels measured in a  
460 non-infected state. This is because the effect of the *cis*-pQTLs upon circulating proteins was estimated in  
461 individuals who had not been exposed to SARS-CoV-2. Once a person contracts SARS-CoV-2 infection,  
462 levels of circulating proteins could be altered and this may be especially relevant for cytokines such as  
463 *IL10* (which binds to *IL10RB*), whose levels may reflect host response to the viral infection and *OAS1*,

464 whose levels are increased by activation of interferon pathway, as we observed in our case-control study  
465 (**Figures S4, S6, S9**). Thus, the MR results presented in this paper should be interpreted as an  
466 estimation of the effect of circulating protein levels, when measured in the non-infected state. On-going  
467 studies will help to clarify if the same *cis*-pQTLs influence circulating protein levels during infection.  
468 Second, this type of study suffers a high false-negative rate. Our goal was not to identify every circulating  
469 protein influencing COVID-19 outcomes, but rather to provide evidence for few proteins with strong *cis*-  
470 pQTLs since these proteins are more likely to be robust to the assumptions of MR studies. Future large-  
471 scale proteomic studies with more circulating proteins properly assayed should help to overcome these  
472 limitations. Third, most MR studies assume a linear relationship between the exposure and the outcome.  
473 Thus, our findings would not identify proteins whose effect upon COVID-19 outcomes has a clear  
474 threshold effect. Finally, we could not completely exclude the possibility that measurement of OAS1 levels  
475 may be influenced by protein altering variants, however, such variants do not affect sQTL RNA-  
476 sequencing studies and the association between OAS1 levels and COVID-19 outcomes remained robust  
477 in such analyses.

478

479 In conclusion, we have used genetic determinants of circulating protein levels and COVID-19 outcomes  
480 obtained from large-scale studies and found compelling evidence that OAS1 has a protective effect on  
481 COVID-19 susceptibility and severity. Measuring OAS1 levels in a case-control study demonstrated that  
482 higher OAS1 levels in a non-infectious state were associated with reduced risk of COVID-19 outcomes.  
483 Interestingly, the available evidence suggests that the protective effect from OAS1 is likely due to the  
484 Neanderthal introgressed p46 OAS1 isoform. Known pharmacological agents that increase OAS1 levels  
485 could be explored for their effect on COVID-19 outcomes.

486

487

488 **Methods:**

489

490 ***pQTL GWAS***

491 We systematically identified pQTL associations from six large proteomic GWASs.<sup>15-20</sup> Each of these  
492 studies undertook proteomic profiling using either SomaLogic® technology, or O-link proximal extension  
493 assays.

494

495 ***COVID GWAS and COVID-19 Outcomes***

496 To assess the association of *cis*-pQTLs with COVID-19 outcomes, we used the largest COVID-19 meta-  
497 analytic GWAS to date from the COVID-19 Host Genetics Initiative<sup>21</sup>. For our study, we used three of  
498 these GWAS meta-analyses which included 25 cohorts of European ancestry and 1 cohort of admixed  
499 American ancestry, based on sample size and clinical relevance. These outcomes were very severe  
500 COVID-19, hospitalization due to COVID-19, and susceptibility to COVID-19 (named A2, B2, and C2,  
501 respectively in the COVID-19 Host Genetics Initiative).

502

503 Very severe COVID-19 cases were defined as hospitalized individuals with COVID-19 as the primary  
504 reason for hospital admission with laboratory confirmed SARS-CoV-2 infection (nucleic acid amplification  
505 tests or serology based), and death or respiratory support (invasive ventilation, continuous positive airway  
506 pressure, Bilevel Positive Airway Pressure, or continuous external negative pressure, high-flow nasal or  
507 face-mask oxygen). Simple supplementary oxygen (e.g. 2 liters/minute via nasal cannula) did not qualify  
508 for case status. Controls were all individuals in the participating cohorts who did not meet this case  
509 definition.

510

511 Hospitalized COVID-19 cases were defined as individuals hospitalized with laboratory confirmed SARS-  
512 CoV-2 infection (using the same microbiology methods as for the very severe phenotype), where

513 hospitalization was due to COVID-19 related symptoms. Controls were all individuals in the participating  
514 cohorts who did not meet this case definition.

515

516 Susceptibility to COVID-19 cases were defined as individuals with laboratory confirmed SARS-CoV-2  
517 infection, health record evidence of COVID-10 (international classification of disease coding or physician  
518 confirmation), or with self-reported infections (e.g. by questionnaire). Controls were all individuals in the  
519 participating cohorts who did not meet this case definition.

520

### 521 ***Two-sample Mendelian randomization***

522 We used two-sample MR analyses to screen and test potential circulating proteins for their role  
523 influencing COVID-19 outcomes. In two-sample MR, the effect of SNPs on the exposure and outcome are  
524 taken from separate GWASs. This method often improves statistical power, because it allows for larger  
525 sample sizes for the exposure and outcome GWAS.<sup>68</sup>

526

527 Exposure definitions: We conducted MR using six large proteomic GWAS studies.<sup>15–20</sup> Circulating  
528 proteins from Sun *et al*, Emilsson *et al* and Pietzner *et al* were measured on the Somalogic platform,  
529 Suhre *et al*, Yao *et al* and Folkersen *et al* used protein measurements on the O-link platform. We selected  
530 proteins with only *cis*-pQTLs to test their effects on COVID-19 outcomes, because they are less likely to  
531 be affected by potential horizontal pleiotropy. The *cis*-pQTLs were defined as the genome-wide significant  
532 SNPs ( $P < 5 \times 10^{-8}$ ) with the lowest P value within 1 Mb of the transcription start site (TSS) of the gene  
533 encoding the measured protein.<sup>9</sup> For proteins from Emilsson *et al*, Pietzner *et al*, Suhre *et al*, Yao *et al*  
534 and Folkersen *et al*, we used the sentinel *cis*-pQTL per protein per study as this was the data available.  
535 For proteins from Sun *et al*, we used PLINK and 1000 genome European population references (1KG  
536 EUR) to clump and select LD-independent *cis*-pQTL ( $R^2 < 0.001$ , distance 1000 kb) with the lowest P-  
537 value from reported summary statistics for each SOMAmer<sup>®</sup> bound proteins. We included the same  
538 proteins represented by different *cis*-pQTLs from different studies in order to cross examine the findings.

539 For *cis*-pQTLs that were not present in the COVID-19 GWAS, SNPs with LD  $R^2 > 0.8$  and with minor allele  
540 frequency (MAF)  $< 0.42$  were selected as proxies, MAF  $> 0.3$  was used for allelic alignment for proxy  
541 SNPs. *cis*-pQTLs with palindromic effects and with minor allele frequency (MAF)  $> 0.42$  were removed  
542 prior to MR to prevent allele-mismatches. Benjamini & Hochberg correction was used to control for the  
543 total number of proteins tested using MR. We recognize that this is an overly conservative correction,  
544 given the non-independence of the circulating proteins, but such stringency should reduce false positive  
545 associations. MR analyses were performed using the TwoSampleMR package in R.<sup>69</sup> For proteins with a  
546 single (sentinel) *cis*-pQTL, we used the Wald ratio to estimate the effect of each circulating protein on  
547 each of the three COVID-19 outcomes. For any proteins/SOMAmer<sup>®</sup> reagents with multiple independent  
548 *cis*-pQTL, an inverse variance weighted (IVW) method was used to meta-analyze their combined effects.  
549 After harmonizing the *cis*-pQTLs of proteins with COVID-19 GWAS, a total of 566 SOMAmer<sup>®</sup> reagents  
550 (529 proteins, 565 directly matched IVs and 26 proxies) from Sun *et al*, 760 proteins (747 directly  
551 matched IVs and 11 proxies) from Emilsson *et al*, 91 proteins (90 directly matched IVs and 2 proxies)  
552 from Pietzner *et al*, 74 proteins (72 directly matched IVs) from Suhre *et al*, 24 proteins (24 directly  
553 matched IVs) from Yao *et al* and 13 proteins (13 directly matched IVs) from Folkersen *et al* were used as  
554 instruments for the MR analyses across the three COVID-19 outcomes (**Table S11-12**).<sup>15–20</sup>

555

### 556 ***Pleiotropy assessments***

557 A common pitfall of MR is horizontal pleiotropy, which occurs when the genetic variant affects the  
558 outcome via pathways independent of circulating proteins. The use of circulating protein *cis*-pQTLs  
559 greatly reduces the possibility of pleiotropy, for reasons described above. We also searched in the  
560 PhenoScanner database, a large catalogue of observed SNP-outcome relationships involving  $> 5,000$   
561 GWAS done to date to assess potentially pleiotropic effects of the *cis*-pQTLs of MR prioritized proteins,  
562 by testing the association of *cis*-pQTLs with other circulating proteins (i.e. if they were *trans*-pQTLs to  
563 other proteins or traits). For *cis*-pQTLs of MR prioritized proteins, if they were measured on SomaLogic<sup>®</sup>  
564 platform, we assessed the possibility of potential aptamer-binding effects (where the presence of protein  
565 altering variants may affect protein measurements). We also checked if *cis*-pQTLs of MR prioritized

566 proteins had significantly heterogeneous associations across COVID-19 populations in each COVID-19  
567 outcome GWAS.

568

### 569 ***Colocalization analysis***

570 Finally, we tested colocalization of the genetic signal for the circulating protein and each of the three  
571 COVID-19 outcomes using colocalization analyses, which assess potential confounding by LD.  
572 Specifically, for each of these MR significant proteins with genome-wide summary data available, for the  
573 proteomic GWASs, a stringent Bayesian analysis was implemented in *coloc* R package to analyze all  
574 variants in 1MB genomic locus centered on the *cis*-pQTL. Colocalizations with posterior probability for  
575 hypothesis 4 (PP4, that there is an association for both protein level and COVID-19 outcomes and they  
576 are driven by the same causal variant) > 0.5 were considered likely to colocalize (which means the  
577 highest posterior probability for all 5 *coloc* hypotheses), and PP4 > 0.8 was considered to be highly likely  
578 to colocalize.

579

### 580 ***sQTL and eQTL MR and colocalization studies for OAS genes***

581 We performed MR and colocalization analysis using GTEx project v8<sup>33</sup> GWAS summary data to  
582 understand the effects of expression and alternative splicing of OAS genes in whole blood. The genetic  
583 instruments were conditionally independent ( $R^2 < 0.001$ ) sQTL and eQTL SNPs for OAS1, eQTL for  
584 OAS2 and OAS3 identified by using stepwise regression in GTEx<sup>33</sup>. The sQTL SNP for OAS1  
585 (rs10774671), was originally identified for the normalized read counts of LeafCutter<sup>31</sup> cluster of the last  
586 intron of p46 isoform (chr12:112,917,700-112,919,389 GRCh38) in GTEx<sup>32</sup>, and was used to estimate the  
587 effect of p46 isoform. Colocalization analysis was performed using GWAS summary from GTEx by  
588 restricting the regions within 1 Mb of rs4767027.

589

### 590 ***Measurement of plasma OAS1 protein levels associated with COVID-19 outcomes in BQC19***

591 BQC19 is a Québec-wide initiative to enable research into the causes and consequences of COVID-19  
592 disease. For this analysis, we used results from patients with available proteomic data from SomaLogic®  
593 assay (**Supplementary Data**). The patients were recruited at the Jewish General Hospital (JGH) and  
594 Centre hospitalier de l'Université de Montréal (CHUM) in Montréal, Québec, Canada.

595  
596 COVID-19 case – control status was defined to be consistent with the GWAS study from COVID-19 HGI,  
597 from which the MR results were derived. Namely, we tested the association of OAS1 protein levels with  
598 the three different COVID-19 outcome definitions both in samples procured from non-infected samples  
599 and from samples during the acute phase of the infection. The three outcomes were: 1) Very severe  
600 COVID-19—defined as hospitalized individuals with laboratory confirmed SARS-CoV-2 infection (nucleic  
601 acid amplification tests or serology based), and death or respiratory support (invasive ventilation,  
602 continuous positive airway pressure, Bilevel Positive Airway Pressure, or continuous external negative  
603 pressure, high flow nasal or face-mask oxygen). Controls were all individuals who did not meet this case  
604 definition; 2) Hospitalized COVID-19 cases—defined as individuals hospitalized with laboratory confirmed  
605 SARS-CoV-2 infection. Controls were all who did not meet this case definition; 3) Susceptibility to COVID-  
606 19—cases were defined as individuals with laboratory confirmed SARS-CoV-2 infection, and controls  
607 were all individuals who underwent PCR testing for SARS-CoV-2, but were negative. The date of  
608 symptom onset for COVID-19 patients was collected from patients' charts or estimated from their first  
609 positive COVID-19 tests if missing. Case inclusion criteria was not exclusive, which means that some  
610 individuals who were cases in the susceptibility analyses were also included in the hospitalization and  
611 very severe COVID-19 if they met case definitions.

612  
613 Among SARS-CoV-2 positive participants, we defined samples procured from participants during the  
614 infectious state as those sampled within 14 days (including the 14<sup>th</sup> day) from the first date of symptoms<sup>70</sup>.  
615 For individuals with more than one sample within 14 days of symptom onset, the earliest sample was  
616 used. We defined samples procured from patients who were non-infectious as samples from SARS-CoV-  
617 2 positive patients taken at least 31 days after symptom onset or from SARS-CoV-2 negative individuals.

618 We selected 31 days, as this is the upper limit of the intra-quartile range of the duration of SARS-CoV-2  
619 positivity in a recent systematic review and coincided with the first scheduled outpatient follow-up blood  
620 test in the BQC19<sup>71</sup>. For individuals with more than one sample at least 31 days of symptom onset, the  
621 latest sample was used. Protein levels in citrated (ACD) plasma samples were measured using the  
622 SomaScan® assay [SomaLogic Inc.]. Details regarding SOMAmer QC are included in **Supplementary**  
623 **Data**.

624

625 1039 samples from 399 SARS-CoV-2 positive patients and 105 SARS-CoV-2 negative patients of mainly  
626 European descent underwent SomaScan® assays, which included 5,284 SOMAmer reagents, targeting  
627 4,742 proteins. A total of 125 individuals were recruited from CHUM and 279 individuals were recruited  
628 from the JGH. Individuals had blood sampling done at up to five different time points (200 individuals had  
629 one measurement, 113 individuals had two measurements, 152 individuals had three measurements, 38  
630 individuals had four measurements and 1 individual had five measurements). Days from symptom onset  
631 were calculated for each sample based on the date of symptom and blood draw date. Sample processing  
632 time (in hours) for each sample was also calculated measure the duration of time from sample collection  
633 to processing to account for the changes in the amount of protein released from cell lysis due to sample  
634 handling time.

635

636 Sample QC was performed to remove outliers with long sample processing time and high OAS1 levels.  
637 OAS1 level was measured by one SOMAmer reagent (OAS1.10361.25). Within each group, normalized  
638 OAS1 levels were natural log transformed, adjusted for sample processing time and the residuals were  
639 further standardized. Logistic regression was performed to test the association standardized OAS1 level  
640 with the three COVID-19 outcomes including age, sex, age<sup>2</sup>, center of recruitment and plates as  
641 covariates.

642

643



644 **Acknowledgements:**

645 We thank Dr. Luis Barriero for his comments on the introgressed Neanderthal p46 isoform, and Dr.  
646 Nicolas Chomont for the discussion on the clinical phenotype of BQC19. We would like to also thank the  
647 MI4 and the MUHC Foundation that contributed for the SomaLogic® panel.

648 **Ethics declarations:**

649 All cohorts contributing cohorts to COVID-19 HGI received ethics approval from their respective research  
650 ethics review boards. The Biobanque Quebecoise de la COVID-19 (BQC19) received ethical approval  
651 from the IRB of JGH and the CHUM.

652 **Data availability:**

653 Data from proteomics studies and GTEx consortium are available from the referenced peer-reviewed  
654 studies or their corresponding authors, as applicable. Summary statistics for the COVID-19 outcomes are  
655 publicly available for download on the COVID-19 HGI website ([www.covid19hg.org](http://www.covid19hg.org)). Applicants are  
656 invited to apply for access to BQC19 data from the JGH hospital ([https://www.mcgill.ca/genepi/mcg-covid-](https://www.mcgill.ca/genepi/mcg-covid-19-biobank)  
657 19-biobank) and/or the BQC19 ([bqc19.ca](http://bqc19.ca)).

658 **Author contributions:**

659 Conception and design: SZ, GBL and JBR. Data analyses: SZ and TN. Data acquisition: TN, GBL, DM,  
660 DEK, JA, MA, LL, EBR, DH, NK, ZA, NR, MB, LP, CG, XX, CT, BV, OA, TA, NA, MC, MD, VF, DEK and  
661 JBR. Interpretation of data: SZ, GBL, TN, MP, YC, DEK, VF and JBR. Funding acquisition: DM, VM, VF,  
662 JBR. Methodology: SZ, KZ, CMTG and JBR. Project administration: DM, VF and JBR. Validation: SZ, TN,  
663 MP, NK, MP, JN, ET, CL, DEK and JBR. Visualization: SZ, TN and VF. Writing-original draft: SZ, GBL,  
664 TN and JBR. Writing-review & editing: SZ, GBL, TN, MP, HZ, VM, MP, RF, ML, MH, CP, DEK and JBR.  
665 All authors were involved in preparation of the further draft of the manuscript and revising it critically for  
666 content. All authors gave final approval of the version to be published. The corresponding author attests  
667 that all listed authors meet authorship criteria and that no others meeting the criteria have been omitted.

**Table 1. MR-Identified Circulating Protein Levels Effecting COVID-19 Outcomes**

Protein	<i>cis</i> -pQTL	Source	Very Severe COVID-19 (99.7% European Ancestry)				Hospitalization (European Ancestry Only)				Susceptibility (European Ancestry Only)			
			OR	95%CI	P value	P het	OR	95%CI	P value	P het	OR	95%CI	P value	P het
OAS1	rs4767027	Sun	0.54	0.44-0.68	$7.0 \times 10^{-8}$	0.37	0.61	0.51-0.73	$8.3 \times 10^{-8}$	0.16	0.78	0.69-0.87	$7.6 \times 10^{-6}$	0.005
ABO	rs505922	Sun, Emilsson	1.09	1.05-1.14	$6.4 \times 10^{-5}$	0.10	1.11	1.07-1.15	$6.8 \times 10^{-9}$	0.06	1.07	1.05-1.10	$1.1 \times 10^{-9}$	0.10
IL10RB	rs2834167	Emilsson	0.47	0.32-0.68	$7.1 \times 10^{-5}$	0.02	0.53	0.39-0.73	$8.8 \times 10^{-5}$	0.11	0.87	0.72-1.07	0.18	0.006

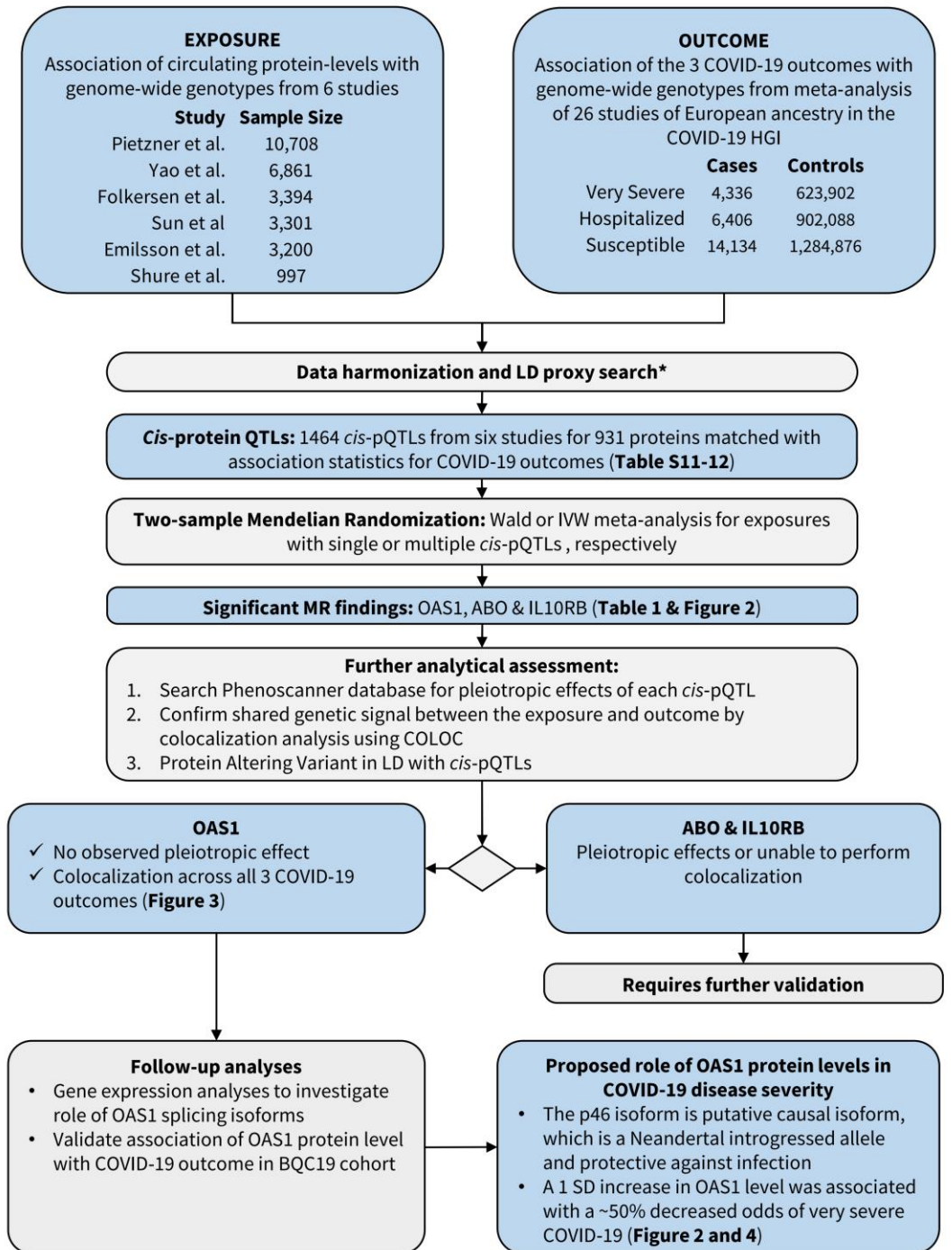
OR: represents the estimated effect of a standard deviation on the natural log scale (for Sun et al) or one unit (for Emilsson et al) increase in protein levels on the odds of the three COVID-19 outcomes. P het: P value of heterogeneity for each *cis*-pQTLs across the cohorts in the GWAS summary-level meta-analysis from COVID-19 Host Genomic Initiative.

**Table 2. Participant demographics for the BQC19 cohort**

<b>Sample Demographics</b>	<b>Total (N=504)</b>
<b>Sex</b>	
Female	250 (49.6%)
Male	254 (50.4%)
<b>Age (years) *</b>	65.4 (18.0)
<b>BMI*</b>	28.6 (6.18)
Missing	225 (44.6%)
<b>SARS-CoV-2 PCR test</b>	
Positive	399 (79.2%)
Negative	105 (20.8%)
<b>Hospitalization</b>	
Hospitalized	406 (80.6%)
Outpatient treatment only	98 (19.4%)
<b>Hospitalization duration (days) †</b>	14.0 [6.00, 27.0]
<b>Death</b>	
Deceased	43 (8.5%)
Survived	461 (91.5%)
<b>Respiratory Support</b>	
No oxygen	233 (46.2%)
Oxygen supplement	143 (28.4%)
Mechanical Ventilation	128 (25.4%)
<b>Days on ventilator †</b>	14.0 [6.75, 23.5]

\* Mean (SD) and † Median (25%QR, 75%QR), which was calculated amongst those who were hospitalized and those on ventilator, respectively.

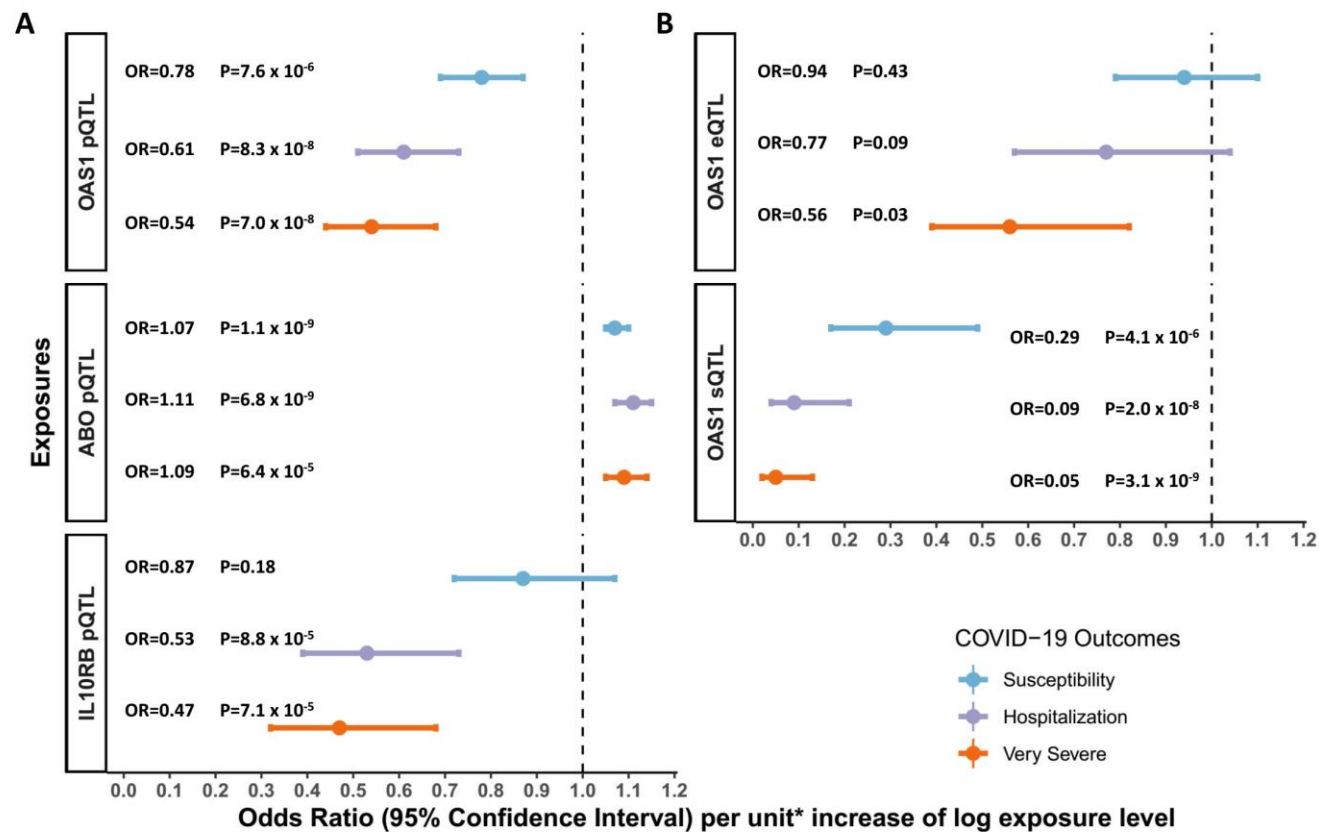
**Figure 1. Flow Diagram of Study Design**



\*A proxy search whereby two distinct genetic variants are considered proxies of each other when they are in high genetic correlation (squared-Pearson correlation > 0.8), a.k.a linkage disequilibrium.

**Legend:** Data Process

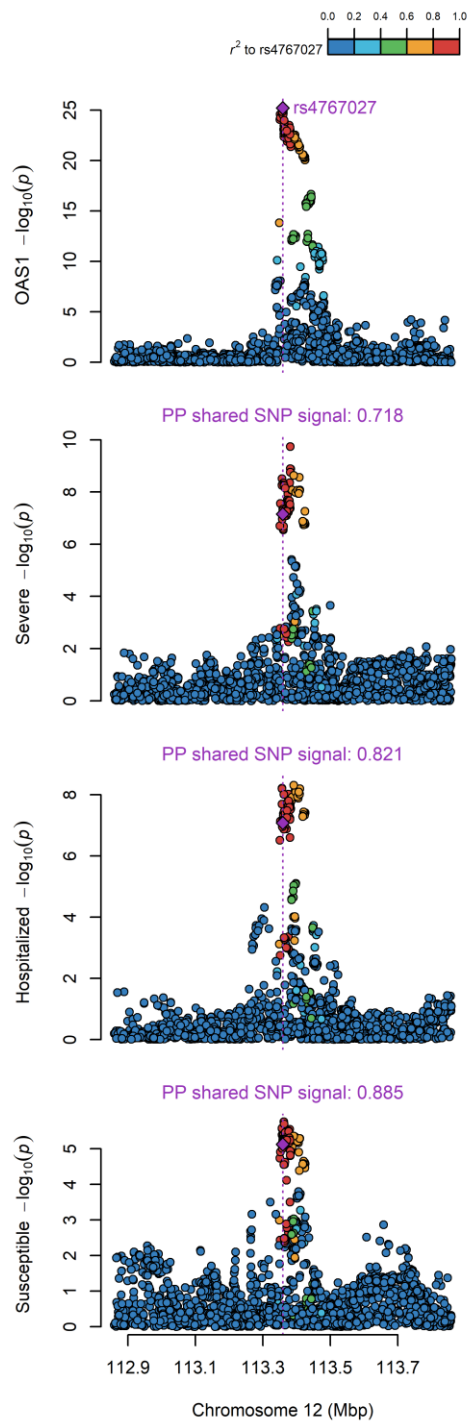
**Figure 2. Association of Circulating Protein Levels of OAS1, ABO and IL10RB and mRNA levels of OAS1 with COVID-19 Outcomes from MR**



A: MR estimates of proteins influencing COVID-19 outcomes, unit: standard deviation of log normalized value;

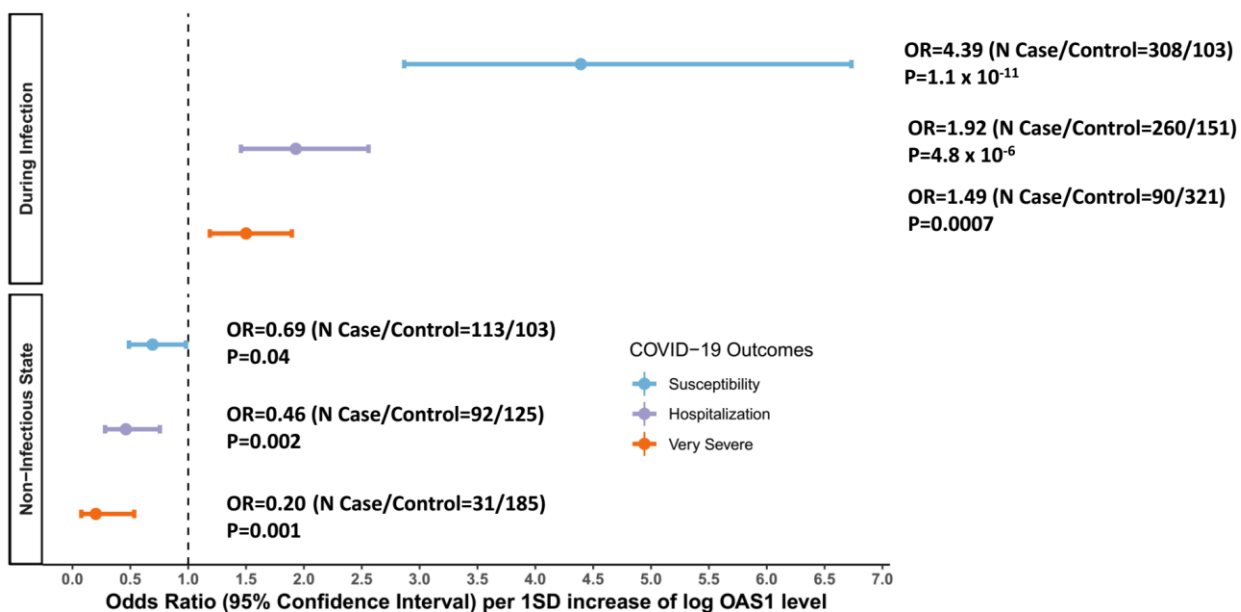
B: MR estimates of OAS1 mRNA influencing COVID-19 outcomes, unit: standard deviation of normalized read counts.

**Figure 3. Colocalization of the Genetic Determinants of OAS1 Plasma Protein Levels and COVID-19 Outcomes**



Colocalization of genetic signal of 1MB region around OAS1 pQTL rs4767027 of OAS1 level (top plot) and COVID-19 outcomes (three bottom plot), color shows SNPs in the region in LD ( $r^2$ ) to rs4767027 (purple). Posterior probability (PP) of shared signal between OAS1 level and three COVID-19 outcomes are estimated by *coloc*.

**Figure 4. Association of OAS1 levels with COVID-19 Outcomes from the Case-Control Study in BQC19**



During Infection: Patient samples that were collected within 14 days from the date of symptom onset. For individuals with two or more samples collected within 14 days of symptom onset, the earliest time point was used.

Non-Infectious State: Patient samples that were collected at least 31 days from the date of symptom onset. For individuals with two or more samples collected at different time points at least 31 days from symptom onset, the latest time point was used.

Additional information is also described in table S10.

## References

1. Johns Hopkins. Corona Virus Resource Center. (2020).
2. David M. Weinreich, M.D., Sumathi Sivapalasingam, M.D., Thomas Norton, M.D., Shazia Ali, Pharm.D., Haitao Gao, Ph.D., Rafia Bhore, Ph.D., Bret J. Musser, Ph.D., Yuhwen Soo, Ph.D., Diana Rofail, Ph.D., Joseph Im, B.S., Christina Perry, M.B.A., Cynthia Pan, B. P. REGN-COV2, a Neutralizing Antibody Cocktail, in Outpatients with Covid-19. *N. Engl. J. Med.* (2020) doi:10.1056/NEJMoa2035002.
3. Dexamethasone in Hospitalized Patients with Covid-19 — Preliminary Report. *N. Engl. J. Med.* 1–11 (2020) doi:10.1056/nejmoa2021436.
4. Sterne, J. A. C. *et al.* Association between administration of systemic corticosteroids and mortality among critically ill patients with COVID-19: A meta-analysis. *JAMA - J. Am. Med. Assoc.* (2020) doi:10.1001/jama.2020.17023.
5. Beigel, J. H. *et al.* Remdesivir for the Treatment of Covid-19 — Preliminary Report. *N. Engl. J. Med.* 2019–2020 (2020) doi:10.1056/nejmoa2007764.
6. Cavalcanti, A. B. *et al.* Hydroxychloroquine with or without Azithromycin in Mild-to-Moderate Covid-19. *N. Engl. J. Med.* (2020) doi:10.1056/nejmoa2019014.
7. Nelson, M. R. *et al.* The support of human genetic evidence for approved drug indications. *Nat. Genet.* **47**, 856–860 (2015).
8. Cook, D. *et al.* Lessons learned from the fate of AstraZeneca’s drug pipeline: a five-dimensional framework. *Nat. Rev. Drug Discov.* **13**, 419–31 (2014).
9. Zheng, J. *et al.* Phenome-wide Mendelian randomization mapping the influence of the plasma proteome on complex diseases. *Nat. Genet.* (2020) doi:10.1038/s41588-020-0682-6.
10. Filbin, M. R. *et al.* Plasma proteomics reveals tissue-specific cell death and mediators of cell-cell interactions in severe COVID-19 patients. *bioRxiv* (2020).
11. Davey Smith, G., Ebrahim, S., Smith, G. D. & Ebrahim, S. ‘Mendelian randomization’: Can genetic epidemiology contribute to understanding environmental determinants of disease? *International Journal of Epidemiology* vol. 32 1–22 (2003).
12. Giambartolomei, C. *et al.* Bayesian Test for Colocalisation between Pairs of Genetic Association Studies Using Summary Statistics. *PLoS Genet.* **10**, (2014).
13. Lawlor, D. A., Tilling, K. & Smith, G. D. Triangulation in aetiological epidemiology. *Int. J. Epidemiol.* (2016) doi:10.1093/ije/dyw314.
14. The COVID-19 Host Genetics Initiative, a global initiative to elucidate the role of host genetic factors in susceptibility and severity of the SARS-CoV-2 virus pandemic. *Eur. J. Hum. Genet.* **28**, 715–718 (2020).
15. Sun, B. B. *et al.* Genomic atlas of the human plasma proteome. *Nature* **558**, 73–79 (2018).
16. Emilsson, V. *et al.* Co-regulatory networks of human serum proteins link genetics to disease. *Science (80-. )*. **1327**, 1–12 (2018).



17. Pietzner, M. *et al.* Genetic architecture of host proteins interacting with SARS-CoV-2. *bioRxiv Prepr. Serv. Biol.* (2020) doi:10.1101/2020.07.01.182709.
18. Folkersen, L. *et al.* Mapping of 79 loci for 83 plasma protein biomarkers in cardiovascular disease. *PLoS Genet.* **13**, e1006706 (2017).
19. Yao, C. *et al.* Genome-wide mapping of plasma protein QTLs identifies putatively causal genes and pathways for cardiovascular disease. *Nat. Commun.* **9**, 3268 (2018).
20. Suhre, K. *et al.* Connecting genetic risk to disease end points through the human blood plasma proteome. *Nat. Commun.* **8**, 14357 (2017).
21. COVID-19 Host Genetics Initiative. <https://www.covid19hg.org/results/>.
22. Erola Pairo-Castineira, Sara Clohisey, Lucija Klaric, Andrew Bretherick, Konrad Rawlik, Nicholas Parkinson, Dorota Pasko, Susan Walker, Anne Richmond, Max Head Fourman, Andy Law, James Furniss, Elvina Gountouna, Nicola Wrobel, Clark D Russell, Loukas Mout, J. K. B. Genetic mechanisms of critical illness in Covid-19. *medrxiv* (2020) doi:<https://doi.org/10.1101/2020.09.24.20200048>.
23. Staley, J. R. *et al.* PhenoScanner: a database of human genotype–phenotype associations. *Bioinformatics* **32**, 3207–3209 (2016).
24. Kristiansen, H. *et al.* Extracellular 2'-5' Oligoadenylate Synthetase Stimulates RNase L-Independent Antiviral Activity: a Novel Mechanism of Virus-Induced Innate Immunity. *J. Virol.* **84**, 11898–11904 (2010).
25. ATGen. <https://nkmaxbio.com/sub/shop.php?ptype=view&prcode=2004011435>.
26. Li, H. *et al.* Identification of a Sjögren's syndrome susceptibility locus at OAS1 that influences isoform switching, protein expression, and responsiveness to type I interferons. *PLoS Genet.* (2017) doi:10.1371/journal.pgen.1006820.
27. Prüfer, K. *et al.* A high-coverage Neandertal genome from Vindija Cave in Croatia. *Science (80- )*. (2017) doi:10.1126/science.aao1887.
28. Meyer, M. *et al.* A high-coverage genome sequence from an archaic Denisovan individual. *Science (80- )*. (2012) doi:10.1126/science.1224344.
29. Sams, A. J. *et al.* Adaptively introgressed Neandertal haplotype at the OAS locus functionally impacts innate immune responses in humans. *Genome Biology* (2016) doi:10.1186/s13059-016-1098-6.
30. Liu, X. *et al.* A functional variant in the OAS1 gene is associated with Sjögren's syndrome complicated with HBV infection. *Sci. Rep.* (2017) doi:10.1038/s41598-017-17931-9.
31. Li, Y. I. *et al.* Annotation-free quantification of RNA splicing using LeafCutter. *Nat. Genet.* (2018) doi:10.1038/s41588-017-0004-9.
32. Aguet, F. *et al.* The GTEx Consortium atlas of genetic regulatory effects across human tissues. *Science (80- )*. (2020) doi:10.1126/SCIENCE.AAZ1776.
33. Aguet, F. *et al.* Genetic effects on gene expression across human tissues. *Nature* **550**, 204–213 (2017).
34. Griffith, G. J. *et al.* Collider bias undermines our understanding of COVID-19 disease risk and severity. *Nat. Commun.* (2020) doi:10.1038/s41467-020-19478-2.

35. Hornung, V., Hartmann, R., Ablasser, A. & Hopfner, K. P. OAS proteins and cGAS: Unifying concepts in sensing and responding to cytosolic nucleic acids. *Nat. Rev. Immunol.* (2014) doi:10.1038/nri3719.
36. Mendez, F. L., Watkins, J. C. & Hammer, M. F. Neandertal origin of genetic variation at the cluster of OAS immunity genes. *Mol. Biol. Evol.* (2013) doi:10.1093/molbev/mst004.
37. Bonnevie-Nielsen, V. *et al.* Variation in antiviral 2',5'-oligoadenylate synthetase (2'5'AS) enzyme activity is controlled by a single-nucleotide polymorphism at a splice-acceptor site in the OAS1 gene. *Am. J. Hum. Genet.* (2005) doi:10.1086/429391.
38. Hugo Zeberg, A. & Pääbo, S. A genetic variant protective for COVID-19 is inherited from Neanderthals. *bioRxiv* (2020).
39. Carey, C. M. *et al.* Recurrent Loss-of-Function Mutations Reveal Costs to OAS1 Antiviral Activity in Primates. *Cell Host Microbe* (2019) doi:10.1016/j.chom.2019.01.001.
40. Zeberg, H. & Pääbo, S. The major genetic risk factor for severe COVID-19 is inherited from Neanderthals. *Nature* (2020) doi:10.1038/s41586-020-2818-3.
41. Schneider, W. M., Chevillotte, M. D. & Rice, C. M. Interferon-Stimulated Genes: A Complex Web of Host Defenses. *Annu. Rev. Immunol.* **32**, 513–545 (2014).
42. Min, J.-Y. & Krug, R. M. The primary function of RNA binding by the influenza A virus NS1 protein in infected cells: Inhibiting the 2'-5' oligo (A) synthetase/RNase L pathway. *Proc. Natl. Acad. Sci. U. S. A.* **103**, 7100–7105 (2006).
43. Hu, B. *et al.* Cellular responses to HSV-1 infection are linked to specific types of alterations in the host transcriptome. *Sci. Rep.* **6**, 28075 (2016).
44. Lim, J. K. *et al.* Genetic Variation in OAS1 Is a Risk Factor for Initial Infection with West Nile Virus in Man. *PLoS Pathog.* **5**, e1000321 (2009).
45. Simon-Loriere, E. *et al.* High Anti-Dengue Virus Activity of the OAS Gene Family Is Associated With Increased Severity of Dengue. *J. Infect. Dis.* **212**, 2011–2020 (2015).
46. Hamano, E. *et al.* Polymorphisms of interferon-inducible genes OAS-1 and MxA associated with SARS in the Vietnamese population. *Biochem. Biophys. Res. Commun.* **329**, 1234–1239 (2005).
47. Di, H., Elbahesh, H. & Brinton, M. A. Characteristics of human OAS1 isoform proteins. *Viruses* (2020) doi:10.3390/v12020152.
48. Cheng, G. *et al.* Pharmacologic Activation of the Innate Immune System to Prevent Respiratory Viral Infections. *Am. J. Respir. Cell Mol. Biol.* **45**, 480–488 (2011).
49. Harari, D., Orr, I., Rotkopf, R., Baranzini, S. E. & Schreiber, G. A robust type I interferon gene signature from blood RNA defines quantitative but not qualitative differences between three major IFN $\beta$  drugs in the treatment of multiple sclerosis. *Hum. Mol. Genet.* **24**, 3192–3205 (2014).
50. Lin, F. ching & Young, H. A. Interferons: Success in anti-viral immunotherapy. *Cytokine and Growth Factor Reviews* (2014) doi:10.1016/j.cytogfr.2014.07.015.
51. Arabi, Y. M. *et al.* Interferon Beta-1b and Lopinavir–Ritonavir for Middle East Respiratory Syndrome. *N. Engl. J. Med.* NEJMoa2015294 (2020) doi:10.1056/NEJMoa2015294.

52. Pan, H. *et al.* Repurposed antiviral drugs for COVID-19 –interim WHO SOLIDARITY trial results. *medRxiv* 2020.10.15.20209817 (2020) doi:10.1101/2020.10.15.20209817.
53. Monk, P. D. *et al.* Safety and efficacy of inhaled nebulised interferon beta-1a (SNG001) for treatment of SARS-CoV-2 infection: a randomised, double-blind, placebo-controlled, phase 2 trial. *Lancet Respir. Med.* (2020) doi:10.1016/S2213-2600(20)30511-7.
54. Wood, E. R. *et al.* The role of phosphodiesterase 12 (PDE12) as a negative regulator of the innate immune response and the discovery of antiviral inhibitors. *J. Biol. Chem.* **290**, 19681–19696 (2015).
55. Poulsen, J. B., Kjær, K. H., Justesen, J. & Martensen, P. M. Enzyme assays for synthesis and degradation of 2-5As and other 2'-5' oligonucleotides. *BMC Biochem.* **16**, 15 (2015).
56. Zhao, L. *et al.* Antagonism of the interferon-induced OAS-RNase L pathway by murine coronavirus ns2 protein is required for virus replication and liver pathology. *Cell Host Microbe* (2012) doi:10.1016/j.chom.2012.04.011.
57. Zhang, R. *et al.* Homologous 2',5'-phosphodiesterases from disparate RNA viruses antagonize antiviral innate immunity. *Proc. Natl. Acad. Sci. U. S. A.* (2013) doi:10.1073/pnas.1306917110.
58. Zhang, Q. *et al.* Inborn errors of type I IFN immunity in patients with life-threatening COVID-19. *Science (80-. )*, **5**, eabd4570 (2020).
59. Verma, R. *et al.* A network map of Interleukin-10 signaling pathway. *J. Cell Commun. Signal.* (2016) doi:10.1007/s12079-015-0302-x.
60. Moreira-Teixeira, L. *et al.* T Cell–Derived IL-10 Impairs Host Resistance to Mycobacterium tuberculosis Infection . *J. Immunol.* (2017) doi:10.4049/jimmunol.1601340.
61. Kasten, K. R., Muenzer, J. T. & Caldwell, C. C. Neutrophils are significant producers of IL-10 during sepsis. *Biochem. Biophys. Res. Commun.* (2010) doi:10.1016/j.bbrc.2010.01.066.
62. Lewkowicz, N. *et al.* Induction of human IL-10-producing neutrophils by LPS-stimulated Treg cells and IL-10. *Mucosal Immunol.* (2016) doi:10.1038/mi.2015.66.
63. Crepaldi, L. *et al.* Up-Regulation of IL-10R1 Expression Is Required to Render Human Neutrophils Fully Responsive to IL-10. *J. Immunol.* (2001) doi:10.4049/jimmunol.167.4.2312.
64. Iyer, S. S., Ghaffari, A. A. & Cheng, G. Lipopolysaccharide-Mediated IL-10 Transcriptional Regulation Requires Sequential Induction of Type I IFNs and IL-27 in Macrophages. *J. Immunol.* (2010) doi:10.4049/jimmunol.1002041.
65. Ray, A., Chakraborty, K. & Ray, P. Immunosuppressive MDSCs induced by TLR signaling during infection and role in resolution of inflammation. *Frontiers in Cellular and Infection Microbiology* (2013) doi:10.3389/fcimb.2013.00052.
66. Petruk, G. *et al.* SARS-CoV-2 Spike protein binds to bacterial lipopolysaccharide and boosts proinflammatory activity. *bioRxiv* (2020).
67. The crucial role of IL-10 in the anti-inflammatory effects of aerobic exercise in a model LPS-induced ARDS. *Eur. Respir. J.* (2013).

68. Burgess, S., Davies, N. M. & Thompson, S. G. Bias due to participant overlap in two-sample Mendelian randomization. *Genet. Epidemiol.* 1–12 (2016) doi:10.1002/gepi.21998.
69. Hemani, G. *et al.* The MR-Base platform supports systematic causal inference across the human phenome. *Elife* **7**, e34408 (2018).
70. Duration of Isolation and Precautions for Adults with COVID-19. <https://www.cdc.gov/coronavirus/2019-ncov/hcp/duration-isolation.html>.
71. Cevik, M. *et al.* SARS-CoV-2, SARS-CoV, and MERS-CoV viral load dynamics, duration of viral shedding, and infectiousness: a systematic review and meta-analysis. *The Lancet Microbe* (2020) doi:10.1016/s2666-5247(20)30172-5.